Measurements of Mass Flux in a Turbulent Liquid Flow with a Chemical Reaction

Satoru Komori, Kouji Nagata, Takao Kanzaki, and Yasuhiro Murakami
Dept. of Chemical Engineering, Kyushu University, Hakozaki, Fukuoka 812, Japan

An original technique for simultaneous measurements of concentration and velocity in a turbulent liquid flow with and without a chemical reaction is developed by combining a two-component He-Ne laser Doppler velocimeter with a Ar^+ laser-induced fluorescence technique. The mass flux and eddy diffusivity of mass are estimated from the simultaneous measurements of concentration and velocity in a liquid shear-free mixing layer downstream of a turbulence grid. The results show that the present measuring technique enables us to simultaneously measure velocity and concentration with high resolutions and that the approximation of the mean gradient diffusion causes about 10% error in estimating the mass flux in a reacting liquid flow.

Introduction

It is of great importance to investigate turbulent mass-transfer mechanism in both estimating the turbulent diffusion of contaminants in the environment and designing industrial combustors and reactors. When a high-order chemical reaction appears in a turbulent flow, the mass-transfer mechanism becomes complicated, since both turbulent mixing and chemical reaction strongly affect the mass-transfer mechanism. One effective way to study the reactive-diffusive mechanism in a reacting flow is to solve numerically both mass transport and Navier-Stokes equations without using assumptions. However, it is very difficult to conduct the direct numerical simulation (DNS) for a reacting liquid flow with high Reynolds and Schmidt numbers, since the minimum scale of the concentration fluctuation, that is, Batchelor scale, is quite small compared to the Kolmogorov scale. Also, huge numerical grid-points are required for the DNS. Thus, the time-averaged mass transport equation has been used for engineering purposes:

$$\frac{\partial \overline{C}}{\partial t}+\overline{U_i}\frac{\partial \overline{C}}{\partial x_i}=\frac{\partial}{\partial x_i}\left(\kappa\frac{\partial \overline{C}}{\partial x_i}-\overline{u_i c}\right)-\overline{R}, \tag{1}$$

where $\overline{C}$ is the mean concentration, $\overline{U_i}$ the mean velocity, c the concentration fluctuation, u_i the velocity fluctuation, κ the molecular diffusivity of mass and $\overline{R}$ is the mean reaction rate. The mean reaction rate for a second-order chemical reaction ($A+B\rightarrow C$) is given by:

$$\overline{R}=k(\overline{C_A}\ \overline{C_B}+\overline{c_A c_B}), \tag{2}$$

where k is the reaction rate constant. To solve the time-averaged equation of Eq. 1, the second-order moments of turbulent fluctuations, $\overline{u_i c}$ and $\overline{c_A c_B}$, must be closed. Here, the moment $\overline{c_A c_B}$ represents the effect of the turbulent mixing on the mean chemical reaction rate. Recently, $\overline{c_A c_B}$ has been directly measured in a reacting liquid flow by using new laser-techniques (Komori et al., 1989a, 1991a), and the effect of the turbulent mixing on the mean reaction rate has been fully discussed by Komori et al. (1991b). However, direct measurements of the mass flux $\overline{u_i c}$ has not been carried out in a reacting liquid flow, since it is very difficult to measure simultaneously instantaneous velocity and concentration with high resolutions comparable to the smallest velocity and concentration scales. Even for a reacting gas flow with the minimum scale of the concentration fluctuation comparable to the Kolmogorov scale, the act of simultaneously measuring the velocity and concentration has been a very difficult task. Therefore, only Bilger et al. (1991) have simultaneously measured the velocity and concentration by combining a hot-wire anemometry and sampling gas analyzers in a reacting gas mixing layer with a second-order chemical reaction. However, their spatial resolution for the

Correspondence concerning this article should be addressed to S. Komori.
Present address of T. Kanzaki: Central Research Institute of Electric Power Industry, Tokyo 201, Japan.

concentration measurements was much larger than the Kolmogorov scale, and an unusual grid-generated turbulence with very low wind-speed and low number of meshes of turbulence grid was used to make the Kolmogorov scale larger.

Thus, there have been few direct measurements of the mass flux in reacting flows, and the mass flux has been generally estimated by the gradient diffusion approximation based on the mean concentration gradient for engineering purposes:

$$\overline{u_i c} = -\epsilon_D \frac{\partial \overline{C}}{\partial x_i} \tag{3}$$

where ϵ_D is the eddy diffusivity of mass for a nonreacting flow. However, the gradient diffusion approximation with the same eddy diffusivity as in a nonreacting flow has been suspected in a reacting flow (Toor, 1991), and both recent direct numerical simulations (for example, Elghobashi and Nomura, 1991) and measurements (Bilger et al., 1991) in reacting gas flows suggest that the concept of the gradient diffusion is collapsed. Though the gradient diffusion approximation is also suspicious for reacting liquid flows which are most common in chemical engineering, the invalidity of the approximation has not been confirmed for a turbulent liquid flow. Furthermore, accurate measurements of concentration statistics in a reacting liquid flow are strongly desired to examine the direct numerical simulations that have been used without the sufficient comparisons with the measurements.

The purpose of this article is, therefore, to present the velocity and concentration statistics by developing an original technique to measure simultaneously the instantaneous velocity and concentration in a turbulent liquid flow with and without a chemical reaction. Secondly, we discuss the mean gradient diffusion approximation for a reacting liquid flow.

The present measuring technique is developed by combining a laser-Doppler velocimeter (LDV) with a laser-induced fluorescence (LIF) technique, and it is applied to the simultaneous measurements of the instantaneous velocity and concentration in a liquid shear-free mixing layer downstream of a turbulence grid with and without a second-order rapid reaction between acetic acid and ammonium hydroxide. To measure simultaneously the velocity and concentration in both reacting and nonreacting liquid flows, the present measuring technique uses two lasers with rather different wavelengths; a He-Ne laser of a 632.8 nm wavelength for LDV and a single-line mode Ar^+ laser of a 488 nm wavelength for LIF. The sodium fluorescein dye sensitive to pH of liquid is used as the fluorescence dye for LIF, and the concentration of a reacting species in a reacting liquid flow is measured using the dependence of the fluorescence on pH (Koochesfahani and Dimotakis, 1986).

On the other hand, Papanicolaou and List (1988) and Barrett and Van Atta (1991) have combined LDV with LIF by using a single multiline mode Ar^+ laser, and they have simultaneously measured the velocity and concentration in a nonreacting liquid flow. The single Ar^+ laser technique requires using the Rhodamine as a fluorescence dye for LIF, since the fluorescence from the Rhodamine has a wavelength around 580 nm (Komori et al., 1989a) which never overlaps with the wavelengths (488 nm and 514.5 nm) of a multiline mode Ar^+ laser for a two-color LDV. However, the Rhodamine is not sensitive to pH of liquid, and it cannot be applied to the concentration measuring technique for a reacting liquid flow, which uses the dependence of the fluorescence on pH. If the sodium fluorescein dye is used with the single Ar^+ laser technique in place of the Rhodamine, the fluorescence from the sodium fluorescein, which has the wavelength rather broadening around 530 nm in the range between 500 and 630 nm, overlaps with the laser Doppler scattering light with the wavelength (514.5 nm) of the green component of a multiline mode Ar^+ laser. This prevented us from using the single Ar^+ laser technique for the present concentration measurements in a reacting liquid flow. Of course, the single laser technique is more convenient for the measurements in a nonreacting liquid flow than the present double laser technique, since the optical arrangement is easier.

Experiments

Figure 1 shows the measuring system and test apparatus. The test apparatus used was the water tunnel which was made of polymethyl methacrylate (PMMA), 1 m in length and 0.1×0.1 m in cross section. The water solutions with A and B species were pumped up from two big storage tanks to the head tanks, and they passed the contraction, which was separated by a splitter plate into two sections. A turbulence grid was installed at the entrance of a test section, and it was of round-rod, square-mesh, single-biplane construction. The mesh size M and the diameter of the rod d were 0.02 and 0.003 m, respectively. Both mean velocities of the nonpremixed A and B streams, $\overline{U}$, were set to the same value of 0.25 m/s, so that a shear-free mixing layer was developed downstream of a turbulence grid. The Reynolds number based on the mesh size was 5,000 and the turbulence Reynolds number was estimated to be 64 at $x/M = 15$. For a nonreacting flow, species A was the solution of the sodium fluorescein dye ($C_{20}H_{10}Na_2O_5$) and species B was the fresh water without other chemical species. The concentration of the sodium fluorescein dye (species A) was 5×10^{-5} mol/m^3. For a reacting flow, a rapid, irreversible, second-order chemical reaction ($CH_3COOH + NH_4OH \rightarrow CH_3COONH_4 + H_2O$) between acetic acid ($CH_3COOH$; species A) and ammonium hydroxide (NH_4OH; species B) was used, and the reaction rate constant was of the order 10^8 m^3/mol•s. The initial concentrations of two reacting species, C_{A0} and C_{B0}, were prepared to the same value of 10 mol/m^3. The sodium fluorescein dye was homogeneously premixed into both the solutions of species A and B at the same concentration of 5×10^{-5} mol/m^3. The combinations of species A and B are listed in Table 1.

The present measuring technique combined a two-component laser-Doppler velocimeter with a laser-induced fluorescence method, as mentioned in the introduction. The laser-Doppler velocimeter used here was a DANTEC 55X Modular system with a polarization beam splitter (55X24), a 40 MHz Bragg cell and a beam expander, and the laser was a 5 mW He-Ne laser with a 632.8 nm wavelength (Spectra Physics Model 106-1). The LDV unit for the velocity measurements was operated in the forward scattering mode, and the reliability of the LDV unit has been confirmed by our previous studies (for example, Komori et al., 1989b,c). For the concentration measurements, a laser-induced fluorescence method was used, and the sodium fluorescein dye in the solution was illuminated by a high-power single-line mode argon-ion (Ar^+) laser of 0.8 W power and a 488 nm wavelength (LEXEL model 95-4). The He-Ne laser beams for the velocity measurements were shot

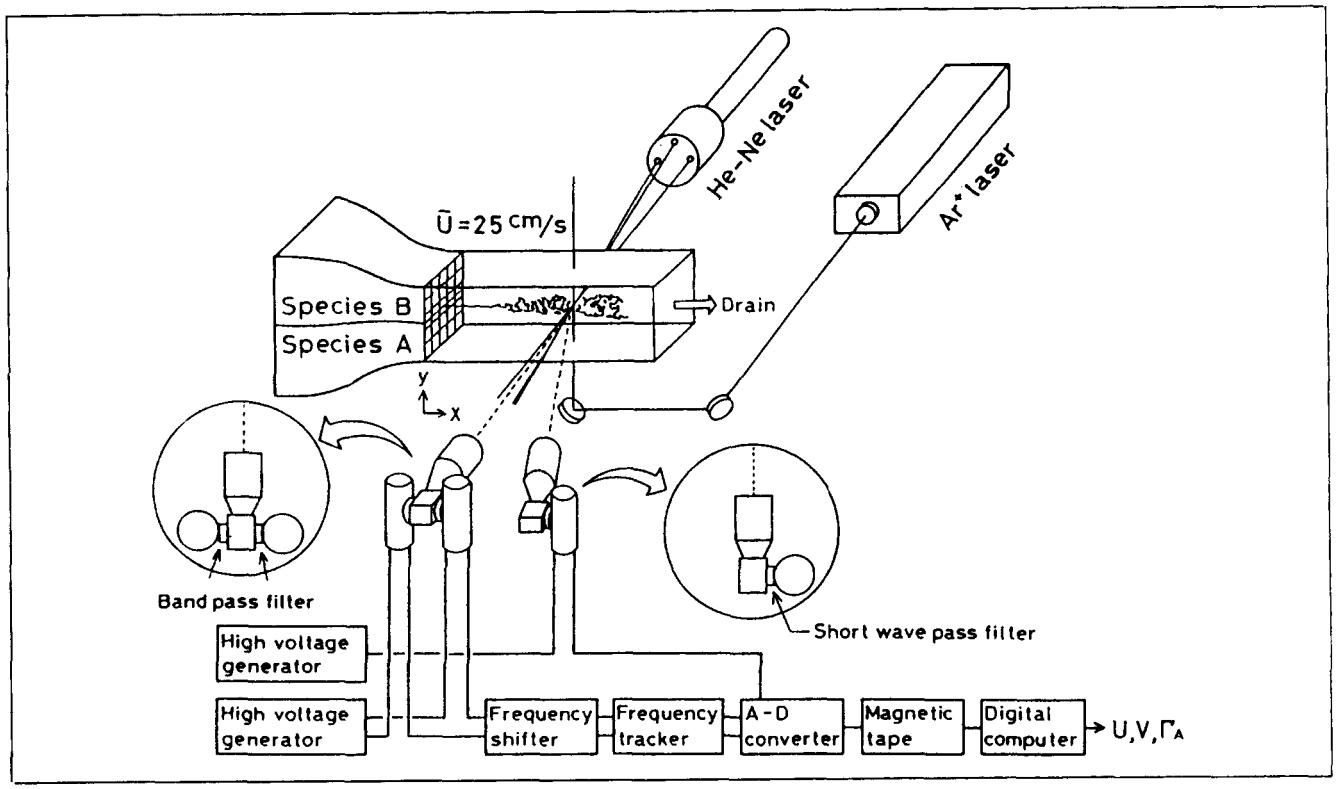

Figure 1. Measuring system and test apparatus.

from the side wall of the test section, and a single-beam of Ar^+ laser was shot from the bottom wall. Both beams were focused by convex lenses and intersected perpendicularly on a measuring point. The fluorescence from the measuring point was collected using the optical system (DANTEC 55X34), which consisted of both a close-up lens of 0.08 m focal length and an objective lens of 0.15 m focal length. The focused and magnified fluorescence passed through a pinhole of 0.1 mm diameter, and it was received by a photomultiplier (Hamamatsu model R-777). The Doppler signals for the velocity measurements were also collected by the optical system (DANTEC 55X34) connected to the photomultipliers (DANTEC 55X08). The wavelength difference between the Doppler signals from the scattered particles and the fluorescence from the sodium fluorescein dye was about 100 nm as shown by the measured spectra in Figure 2, and therefore the two lights could be separated by installing optical filters between the optical system and the photomultiplier. The shortwave and bandwave pass filters, which were specially made, were installed in front of the photomultipliers for the concentration and velocity measurements, respectively, and the transmittances of the filters

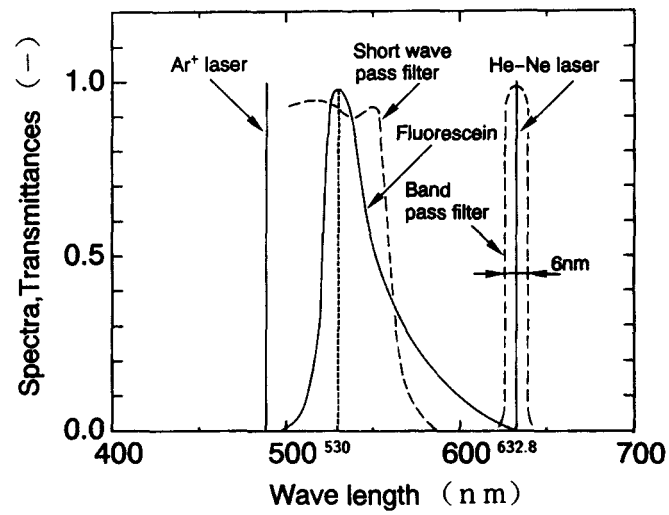

Figure 2. Measured spectra of fluorescence and scattering lights and transmittances of shortwave and bandwave pass filters.

Table 1. Combinations of Species A and B

	Species *A*	Species *B*	Reaction Rate Constant
Nonreacting Case	Fluorescein	—	0
Reacting Case	Acetic Acid + Fluorescein	Ammonium Hydroxide + Fluorescein	10^8 m^3/mol•s

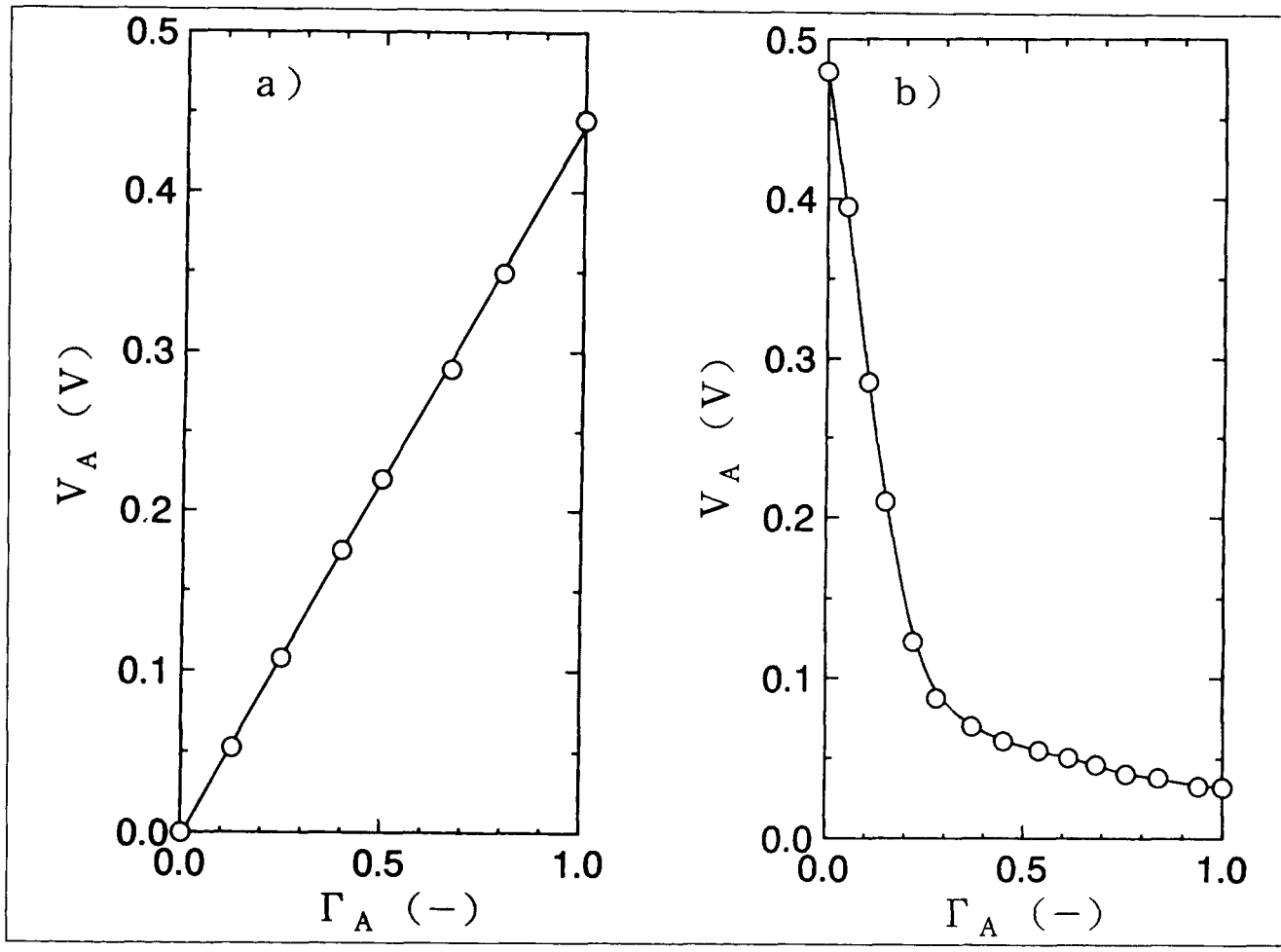

Figure 3. Calibration curves between concentration of species *A* and voltage output from a photomultiplier.
(a) Nonreacting case; (b) Reacting case.

are also shown in Figure 2. The measurements were made in the region of $6 \leq x/M \leq 20$ in a shear-free mixing layer.

Figure 3 shows the calibration curves between the concentration of species A and the voltage output from the photomultiplier, which were measured in a well mixed calibration tank with the dimensions of $0.1 \times 0.1 \times 0.1$ m. For a nonreacting case, the intensity of the fluorescence is clearly proportional to the concentration of the fluorescein dye and therefore the measurements of the concentration of species A can easily be attained by measuring the intensity of the fluorescence. For a reacting case, the intensity of the fluorescence is constant in the region of $pH \geq 7$, but it strongly depends on the pH of the solution on the measuring point in the region of $pH < 7$. To measure the concentration of species A (acetic acid) by using the nonlinear calibration curve in Figure 3b, the measuring volume for the concentration measurements should, therefore, be comparable to or smaller than the smallest concentration scale (that is, Batchelor scale).

Results and Discussion

Reliability of concentration measuring technique

The accuracy of the present concentration measuring technique depends on two problems of the optical separation and spatial resolution. The reliability of the optical separation, that is, the interference effect between the fluorescence and scattering lights, was estimated by comparing the rms values of the concentration and velocity fluctuations simultaneously measured by using both He-Ne and Ar^+ lasers with the rms values separately measured by using each laser. The results showed that the rms values do not at all change between the simultaneous and separate measurements and that the interference effect of the laser beams can be disappeared by the optical wave pass filters shown in Figure 2.

To estimate the measuring volume for the concentration measurements, the power spectrum of the concentration fluctuation measured on the centerline at $x/M = 20$ in a nonreacting flow was calculated. The spectrum normalized by the mean squared value of concentration fluctuation is shown in Figure 4. The spectrum shows the broadening in the high frequency region. The frequency limit due to the broadening is about 2,100 Hz as indicated by a dashed line, and it corresponds to the spatial scale of 19 μm. The spatial scale is rather smaller than the Kolmogorov scale of about 350 μm, and it is comparable to the Batchelor scale of about 15 μm. This means that the spatial resolution of the present technique is sufficient for the concentration measurements.

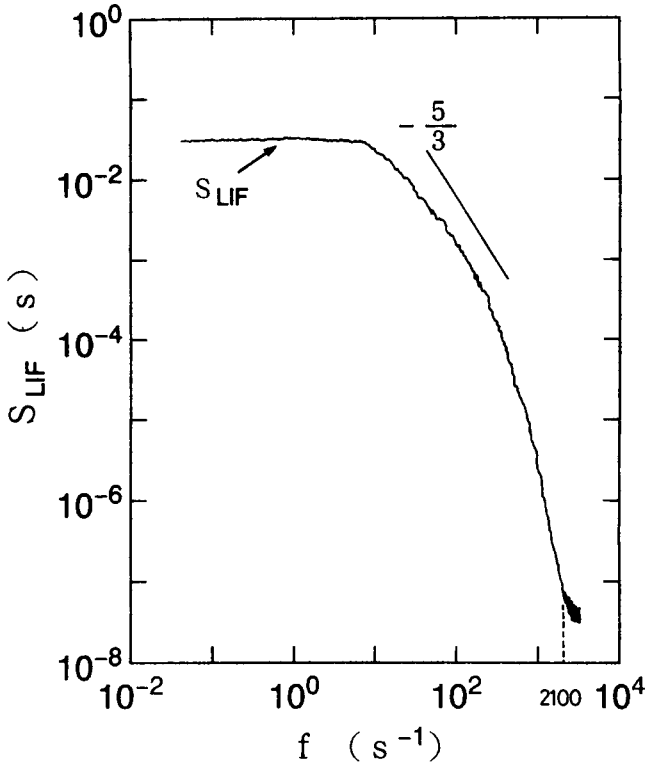

Figure 4. Power spectrum of concentration fluctuation measured on the centerline of the test section at $x/M = 20$ in a nonreacting flow.

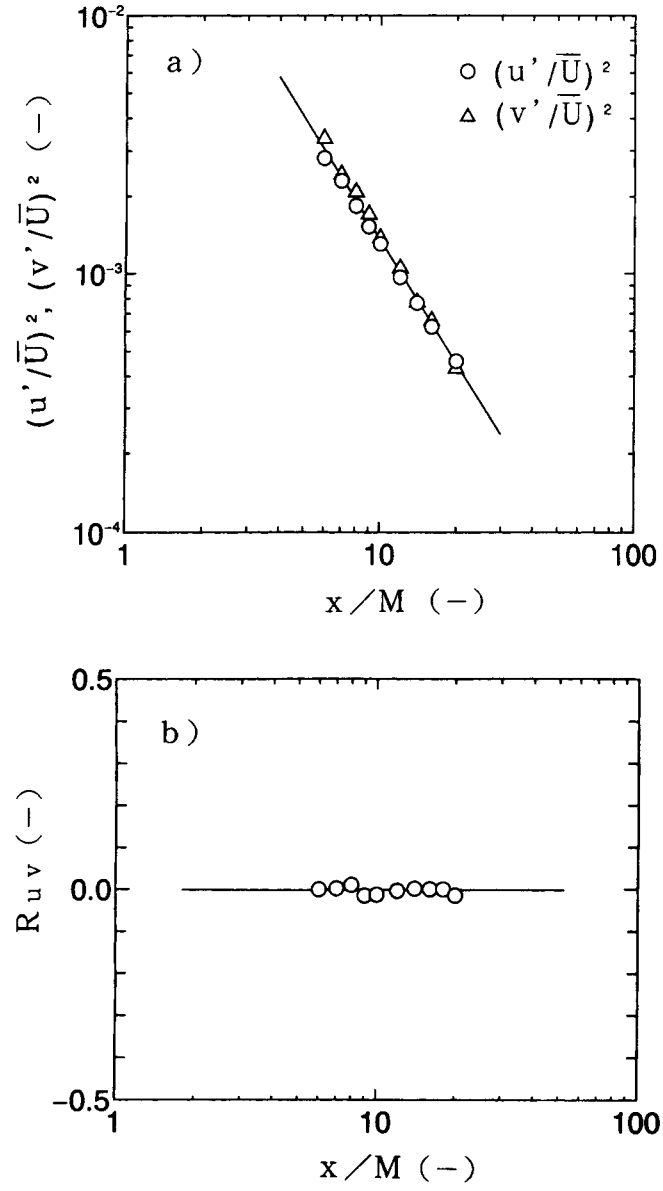

Figure 5. Longitudinal variations of the squared turbulence intensities and the correlation coefficient between longitudinal and transverse velocity fluctuations.

(a) Squared turbulence intensities; (b) Correlation coefficient.

Turbulence quantities

Figure 5 shows the decay of the velocity fluctuations downstream of a turbulence grid and the longitudinal variation of the correlation coefficient between the longitudinal (streamwise) and transverse velocity fluctuations measured on the centerline of the test section. The decay of the squared turbulent intensities measured on the centerline of the test section is approximated by:

$$u'^2/\overline{U}^2 = v'^2/\overline{U}^2 = 0.0556\ (x/M)^{-1.59}, \tag{4}$$

where u' and v' are the rms values of the longitudinal and transverse velocity fluctuations u and v. The correlation coefficient $R_{uv}(=-\overline{uv}/u'v')$ is almost equal to zero in the whole region. The results show that an ideal grid-generated turbulence is produced in the present test section downstream of a turbulence grid.

Figure 6 shows the longitudinal and transverse profiles of the mean concentration of species A, $\overline{\Gamma_A}$. Here, the concentration Γ_A is normalized by the value of the initial concentration C_{A0}. The mean concentration on the centerline of the test section is constant against x/M in a nonreacting flow, but in a reacting flow it drastically decreases in the region of $x/M < 10$ where the chemical reaction rapidly progresses. The transverse profiles also show the drastic progress of the chemical reaction in the central region near $y/M = 0$.

Figure 7 shows the normalized mean-squared values of concentration fluctuation of species A, $\gamma_A'^2 (= c_A'^2/C_{A0}^2)$. The mean-squared value on the centerline in a nonreacting flow decays downstream:

$$\gamma_A'^2 = 0.325\ (x/M)^{-0.331}. \tag{5}$$

This decay is rather slower than that of scalar in a similar gas flow with a low Schmidt number (for example, LaRue and Libby, 1981; Elghobashi and Launder, 1983). The values of $\gamma_A'^2$ in a reacting flow are a little larger than those in a nonreacting flow, since species A mixed by the molecular diffusion is consumed by the chemical reaction and the reaction makes the time-variations of the concentration fluctuation sharper than in a nonreacting flow. The transverse distributions of $\gamma_A'^2$ are symmetric with respect to the transverse y axis in a

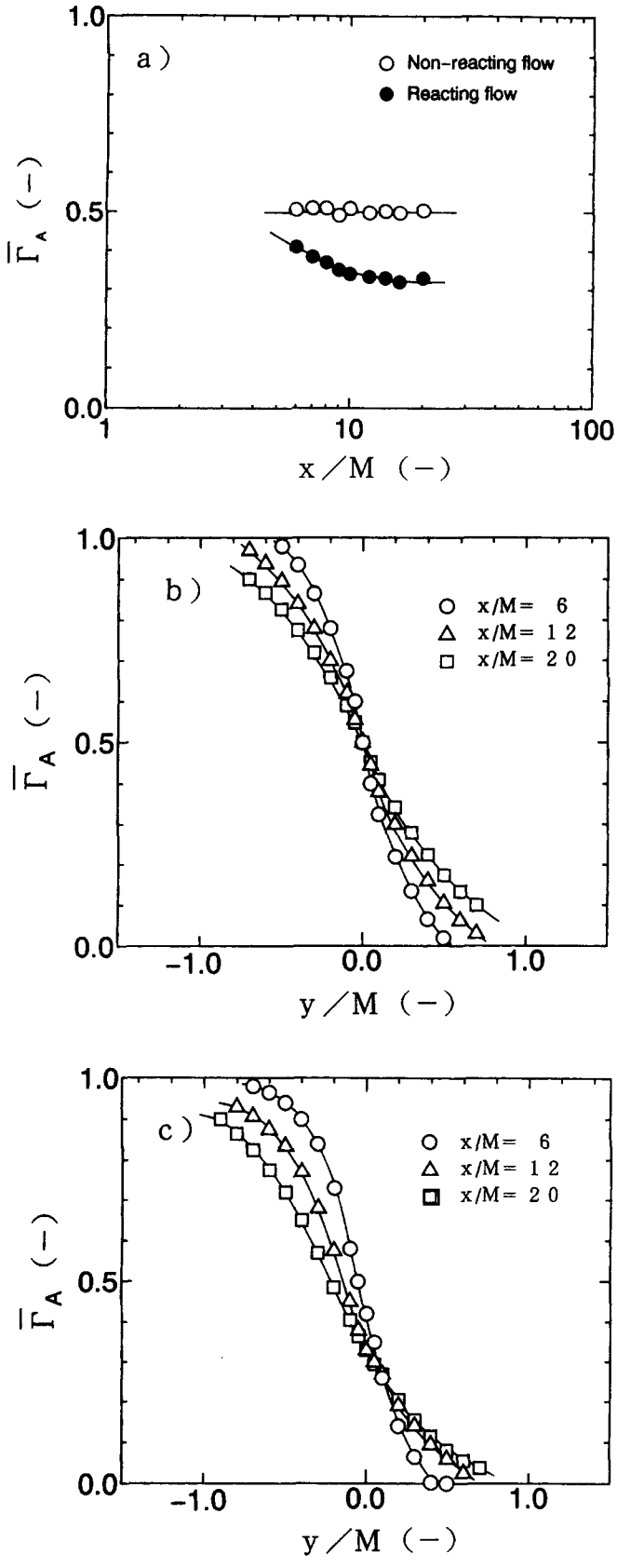

Figure 6. Longitudinal and transverse profiles of the mean concentration of species A.

(a) Longitudinal profiles; (b) Transverse profiles in a nonreacting flow; (c) Transverse profiles in a reacting flow.

nonreacting flow, but in a reacting flow they become asymmetric because of the reaction.

Figure 8 shows the longitudinal and transverse profiles of the normalized mass flux in the transverse (y) direction, $\overline{v^*\gamma_A}$. Here, v^* and γ_A are given by $v/\overline{U}$ and c_A/C_{A0}, respectively. The normalized mass flux $\overline{v^*\gamma_A}$ on the centerline of the test section in a nonreacting flow is approximated by

$$\overline{v^*\gamma_A} = 0.069\ (x/M)^{-1}. \tag{6}$$

This well agrees with the relation derived under the assumption of the self-preservation, and the agreement supports the reliability of the present technique for the simultaneous measurements of velocity and concentration. For a reacting case, the mass flux becomes a little smaller than that for a nonreacting case, since the correlation between v^* and γ_A is weakened by the chemical reaction. The transverse profile of $v^*\gamma_A$ in a nonreacting flow is symmetric with respect to the y axis, but the symmetry is collapsed in a reacting flow as well as in the profiles of $\gamma_A{}'^2$. Especially, it should be noted that the symmetry in a nonreacting flow also supports the reliability of the present measuring technique. The longitudinal mass flux was negligibly small, compared to the transverse one, and it was not presented here. Further, the measurements of the mass flux enable us to estimate the mean reaction rate $\overline{R}$ in Eq. 1 by:

$$\overline{R} = -\frac{\partial}{\partial y}\left(\overline{vc_A}\right) - \overline{U}\,\frac{\partial \overline{C_A}}{\partial x}, \tag{7}$$

since $\overline{V}$, $\overline{W}$, and $\overline{uc_A}$ in Eq. 1 are equal to zero. The longitudinal profile of the mean reaction rate is shown in Figure 9. Here the mean reaction rate $\overline{R}^*$ is normalized by $\overline{U}C_{A0}/M$. It is found that the chemical reaction rapidly progresses in the region of $x/M < 10$, as suggested by Γ_A in Figure 6.

To inspect the validity of the gradient diffusion approximation for the mass flux in a reacting flow, the eddy diffusivity of mass was calculated from both the transverse gradient of mean concentration and the transverse mass flux. Figure 10a shows the variation of the normalized eddy diffusivity of mass, ϵ_D^* ($=\epsilon_D/\overline{U}M$), against x/M. In the region of $x/M < 10$ where the chemical reaction rapidly progresses (see Figures 6 and 9), the eddy diffusivity in a reacting flow is a little larger than that in a nonreacting flow. This is attributed to that the mean concentration gradient in the transverse direction becomes sharper by the reaction than in a nonreacting flow. The difference is about 10%, and it shows that the gradient diffusion approximation gives about 10% error in estimating the mass flux in a reacting liquid flow. The transverse profiles of ϵ_D^* at $x/M = 12$ are shown in Figure 10b. In the central region of $-0.25 \le y/M \le 0.25$ where the mean concentration gradient and mass flux can accurately be estimated, the eddy diffusivity ϵ_D^* is almost constant in the transverse direction. In the outer region of $y/M > 0.25$ and $y/M < -0.25$ the values of ϵ_D^* slightly decrease with increasing y/M. However, the estimated values of ϵ_D^* in the outer region may be unreliable because of the small mean concentration gradient. On the other hand, the results of Bilger et al. (1991), which were obtained in a reacting gas flow with a similar concentration field, are quite different from the present results. Bilger et al. (1991) showed that the eddy diffusivity strongly varies in the transverse direction even in

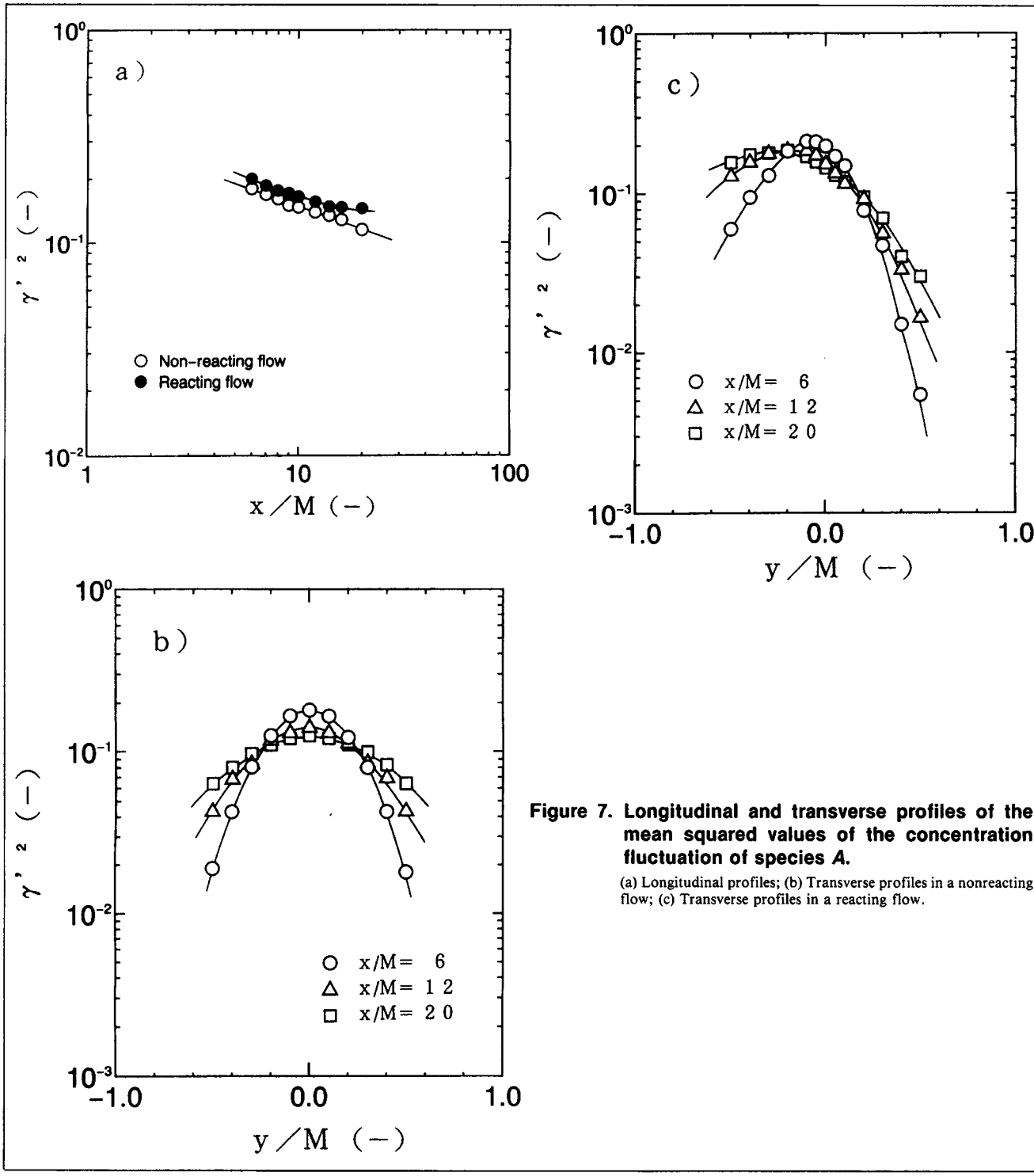

Figure 7. Longitudinal and transverse profiles of the mean squared values of the concentration fluctuation of species *A*.

(a) Longitudinal profiles; (b) Transverse profiles in a nonreacting flow; (c) Transverse profiles in a reacting flow.

the central region with the large mean concentration gradient. The difference may suggest that the gradient diffusion approximation is rather collapsed in a reacting gas flow of Bilger et al. (1991).

Conclusions

Simultaneous measurements of the velocity and concentration were carried out in a liquid shear-free mixing layer downstream of a turbulence grid, and the velocity and concentration statistics were estimated for both reacting and nonreacting cases. The results from this article can be summarized as follows.

- An original technique for simultaneous measurements of the instantaneous velocity and concentration for both reacting and nonreacting liquid flows was developed, and it enabled us to measure the turbulent mass flux and other quantities with a high accuracy.

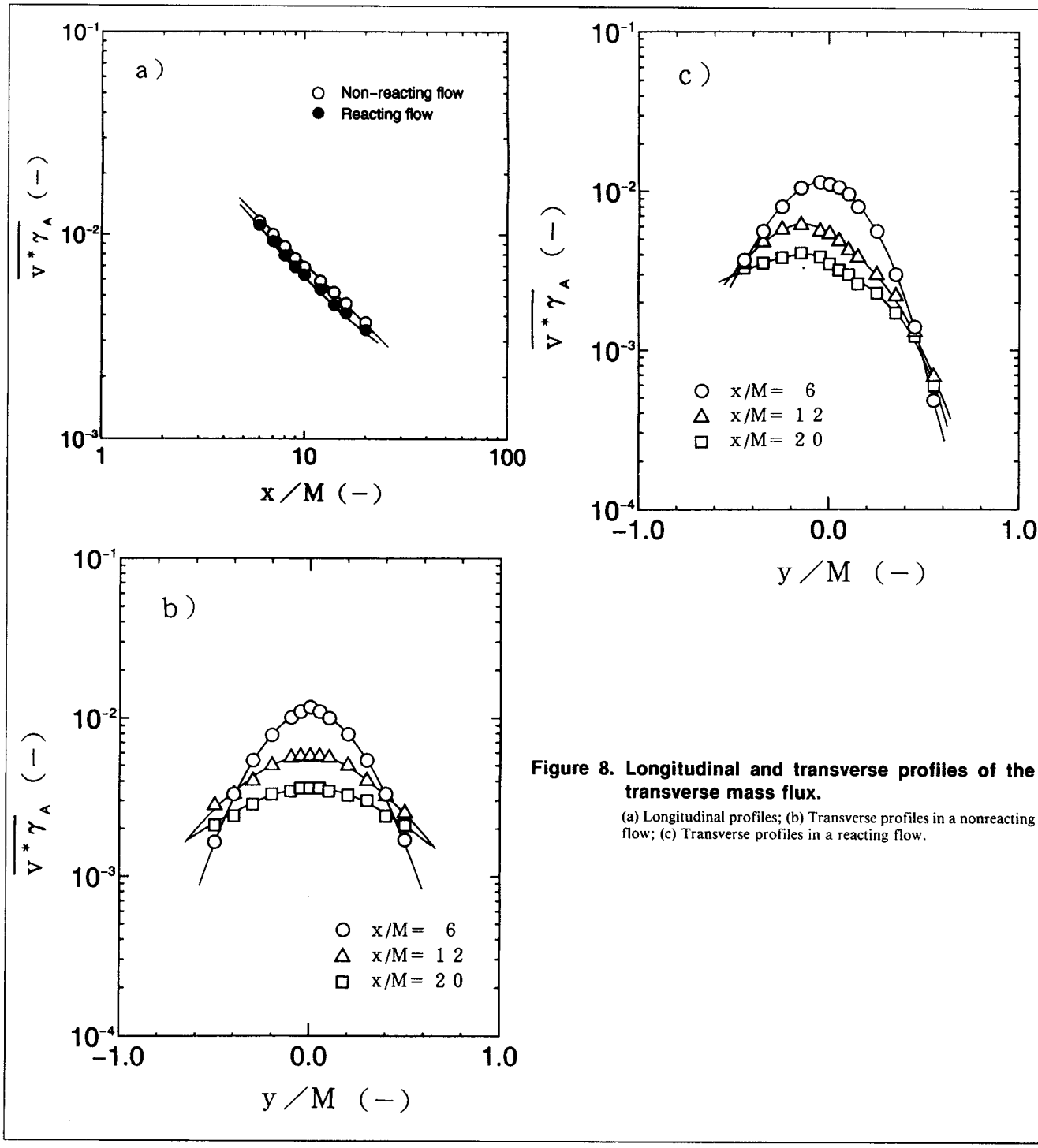

Figure 8. Longitudinal and transverse profiles of the transverse mass flux.

(a) Longitudinal profiles; (b) Transverse profiles in a nonreacting flow; (c) Transverse profiles in a reacting flow.

- The mean squared values of the concentration fluctuation in a reacting flow are larger than those in a nonreacting flow, and they become asymmetric in the transverse direction in a reacting flow. The transverse mass flux in a reacting flow also shows the asymmetric transverse profile, but it is smaller than that in a nonreacting flow.
- The eddy diffusivity of mass decays in the downstream direction in both reacting and nonreacting flows, and it is almost constant in the transverse direction. However, the eddy diffusivity in a reacting flow is a little larger than that in a nonreacting flow, and the fact shows that the gradient diffusion approximation gives about 10% error in estimating the mass flux in a reacting liquid flow.

Acknowledgment

The authors acknowledge the financial support for this study by the Japanese Ministry of Education under Grant No. 03555039. They also thank Kouji Kondo for his help in conducting experiments.

Notation

c = concentration fluctuation

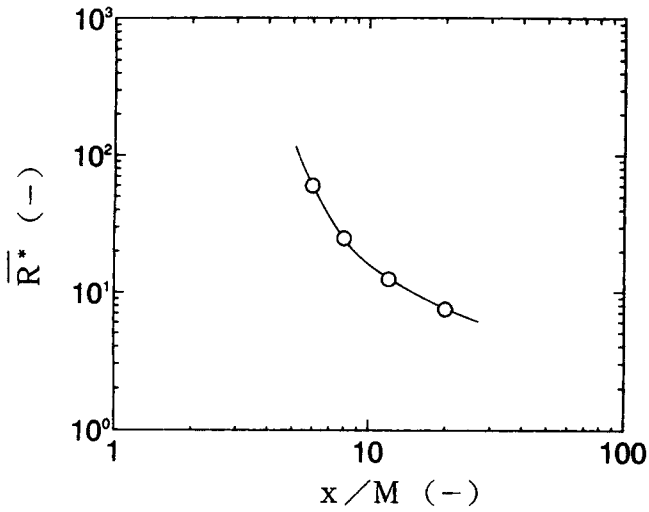

Figure 9. Longitudinal profile of the mean reaction rate in a reacting flow.

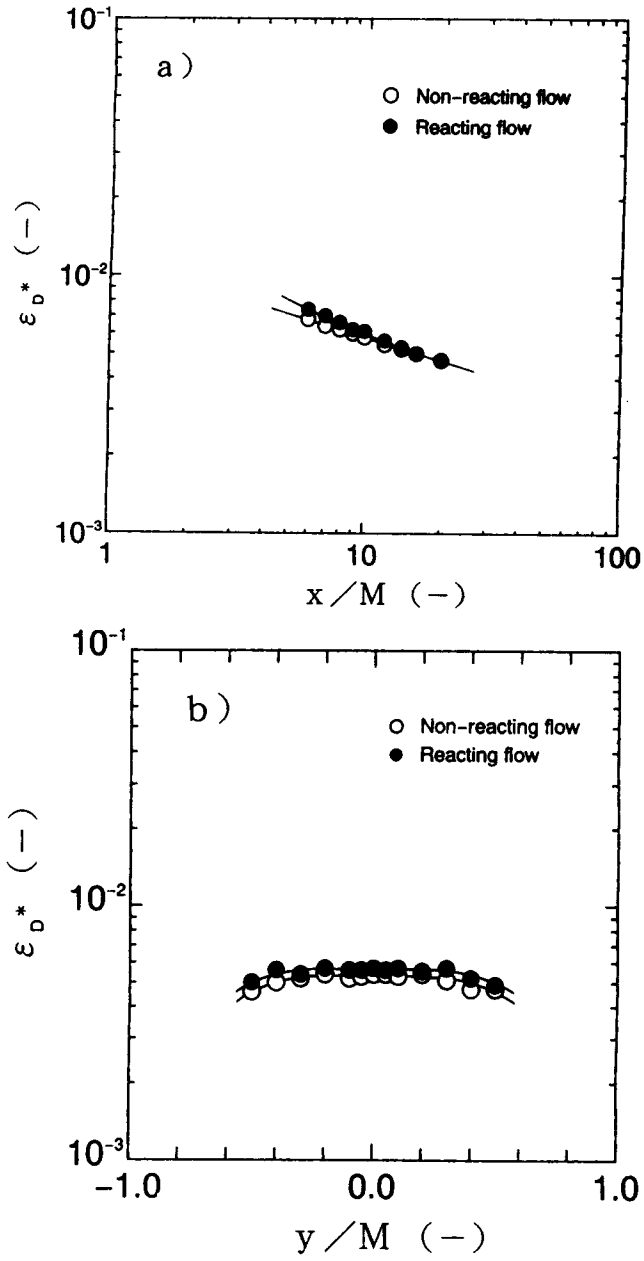

Figure 10. Longitudinal and transverse profiles of eddy diffusivity of mass.

(a) Longitudinal profiles; (b) Transverse profiles at $x/M = 12$.

C = instantaneous concentration
k = reaction rate constant
M = mesh size of a turbulence grid
R = instantaneous reaction rate in Eq. 2
R^* = normalized mean reaction rate $= RM/\overline{U}C_{A0}$
R_{uv} = correlation coefficient between u and $v = -\overline{uv}/u'v'$
U = instantaneous velocity in the longitudinal x-direction
U_i = instantaneous velocity in the i-direction
u = velocity fluctuation in the longitudinal x-direction
u_i = velocity fluctuation in the i-direction
v = velocity fluctuation in the transverse y-direction
v^* = normalized velocity fluctuation $= v/\overline{U}$
V = instantaneous velocity in the transverse y-direction
W = instantaneous velocity in the z-direction
x = space coordinate in the longitudinal (streamwise) direction or longitudinal distance from a turbulence grid
x_i = space coordinate in the i-direction
y = space coordinate in the transverse direction or transverse distance from the centerline of the test section
z = space coordinate in the lateral direction

Greek letters

γ = normalized concentration fluctuation $= c/C_0$
Γ = normalized concentration $= C/C_0$
ϵ_D = eddy diffusivity of mass
ϵ_D^* = normalized eddy diffusivity of mass $= \epsilon_D/\overline{U}M$
κ = molecular diffusivity of mass

Subscripts

A = species A
B = species B
0 = initial value

Other symbols

$\_'$ = rms value
$\overline{\_}$ = time-averaged value

Literature Cited

Barrett, T. K., and C. W. Van Atta, "Experiments on the Inhibition of Mixing in Stably Stratified Decaying Turbulence Using Laser Doppler Anemometry and Laser-Induced Fluorescence," *Phys. Fluids A*, 3, 1321 (1991).

Bilger, R. W., L. R. Saetran, and L. V. Krishnamoorthy, "Reaction in a Scalar Mixing Layer," *J. Fluid Mech.*, **233**, 211 (1991).

Elghobashi, S. E., and B. E. Launder, "Turbulent Time Scales and the Dissipation Rate of Temperature Variance in the Thermal Mixing Layer," *Phys. Fluids*, **26**, 2415 (1983).

Elghobashi, S., and K. K. Nomura, "Direct Simulation of a Passive Diffusion Flame in Sheared and Unsheared Homogeneous Turbulence," *Turbulent Shear Flow 7*, F. J. Durst, B. E. Launder, F. W. Schmidt, and J. H. Whitelaw, eds., Springer, p. 313 (1991).

Komori, S., J. C. R. Hunt, T. Kanzaki, and Y. Murakami, "The Effects of Turbulent Mixing on the Correlation Between Two Species and on Concentration Fluctuations in Non-Premixed Reacting Flows," *J. Fluid Mech.*, **228**, 629 (1991b).

Komori, S., T. Kanzaki, and Y. Murakami, "Simultaneous Measurements of Instantaneous Concentrations of Two Reacting Species in a Turbulent Flow with a Rapid Reaction," *Phys. Fluids A*, 3, 507 (1991a).

Komori, S., T. Kanzaki, Y. Murakami, and H. Ueda, "Simultaneous Measurements of Instantaneous Concentrations of Two Species Being Mixed in a Turbulent Flow by Using a Combined Laser-Induced Fluorescence and Laser-Scattering Technique," *Phys. Fluids A*, **1**, 349 (1989a).

Komori, S., Y. Murakami, and H. Ueda, "The Relationship Between Surface-Renewal and Bursting Motions in an Open-Channel Flow," *J. Fluid Mech.*, **203**, 103 (1989b).

Komori, S., Y. Murakami, and H. Ueda, "Detection of Coherent Structures Associated with Bursting Events in an Open-Channel Flow by a Two-Point LDV-Measuring Technique," *Phys. Fluids A*, **1**, 339 (1989c).

Koochesfahani, M. M., and P. E. Dimotakis, "Mixing in a Turbulent Liquid Mixing Layer," *J. Fluid Mech.*, **170**, 83 (1986).

LaRue, J. C., and P. A. Libby, "Thermal Mixing Layer Downstream of Half-Heated Turbulence Grid," *Phys. Fluids*, **24**, 597 (1981).

Papanicolaou, P. N., and E. J. List, "Investigations of Round Vertical Turbulent Buoyant Jets," *J. Fluid Mech.*, **195**, 341 (1988).

Toor, H. L., "Turbulent Diffusivities in Reacting Systems," *AIChE J.*, **37**, 1737 (1991).

Manuscript received Sept. 24, 1992, and revision received Feb. 9, 1993.